CHROMOPHORIC DISSOLVED ORGANIC MATTER IN COASTAL RAINWATER

Kelly Jo Gordon

A Thesis Submitted to the
University of North Carolina at Wilmington in Partial Fulfillment
Of the Requirements for the Degree of
Master of Science

Department of Chemistry

University of North Carolina at Wilmington

2007

Approved by

Advisory Committee

Carrie Miller	Pamela Seaton
Joan Willey	Robert Kieber Chair

Accepted by

_____
Dean, Graduate School

TABLE OF CONTENTS

ABSTRACT

Chromophoric dissolved organic matter (DOM) was measured in 37 rain events in Wilmington, NC, between September 15, 2005 to September 6, 2006. Each rain event was analyzed via 3D fluorescence, UV-Vis absorption spectroscopy, nuclear magnetic resonance (NMR) spectroscopy, and dissolved organic carbon measurements were acquired. All rain events had measurable CDOM, although there was much variability between events.

Chromophoric DOM was found in both the C_{18} extract (hydrophobic) and the C_{18} filtrate (hydrophilic) fraction, but surprisingly a large fraction of the chromophoric DOM is relatively hydrophilic (~50%). Using NMR, it was determined that in all rain events the majority of the protons were alkyl. A strong positive correlation was found between the fluorescence and the overall integration of the NMR spectra. A correlation was also found between fluorescence and the various integral regions of the NMR with the greatest contribution to fluorescence coming from the aromatic region.

The abundance and characteristics of rainwater DOM was affected by season and storm origin. Marine storms contained a larger percentage of aromatic protons relative to the terrestrial storms. This coupled with lower spectral slopes and a higher percentage fluorescence in the C_{18} extract samples from marine storms suggests that while the dissolved organic carbon (DOC) concentrations in these storms are low, the DOM in marine storms likely contains recalcitrant DOM which is globally distributed. The composition of DOM in rainwater is also influenced by season. Samples collected during the warm season had lower spectral slopes and lower percent DOC in the reconstituted fraction which suggests that warm season storms contain smaller molecular weight DOM. This is a result of photodegredation during the warm season.

ACKNOWLEDGMENTS

I would like to thank my research committee Dr. Robert Kieber, Dr. Joan Willey, and Dr. Pam Seaton for their patience, support and guidance. Special thanks go to Dr. Carrie Miller and Carter Crowl for their friendship and always being there. I could not have written this thesis with such ease if it wasn't for Dr. Miller. As for Carter, there is no way I could have produced so much data with the efficiency and accuracy that we did without him. I want to thank Carter and Dr. Miller for listening to me stress and telling me that I could do it when I didn't think that there was an end in sight. I appreciate the opportunity to work with a wide variety of members of MACRL and the UNCW staff. To my mother, sister, and brother, thanks for putting up with the years of college that I have endured and have left to endure. I could not have accomplished this and all that I have without them.

LIST OF TABLES

LIST OF FIGURES

INTRODUCTION

Dissolved organic matter (DOM) is a ubiquitous, integral component of Wilmington, North Carolina, rainwater. The presence of significant quantities of highly chromophoric DOM in atmospheric waters has profound ramifications with respect to a wide variety of fundamental processes in atmospheric chemistry because of its impact on solar radiative transfer and its involvement in the oxidizing and acid generating capacity of the troposphere. Additionally, if DOM constituents are surface-active they will have a direct impact on droplet population and consequently cloud albedo by lowering the surface tension of atmospheric waters.

Previous studies have only been able to identify less than 50% of the organic compounds in rainwater (Willey et al. 2000). DOM is by far the dominant chromophore in rainwater with the UV-Vis absorbance of samples decreasing exponentially between 250 to 550 nm and as such plays a vital role in light attenuation in atmospheric waters. Recent research has also revealed a strong positive correlation between total integrated fluorescence and absorbance coefficient at 300 nm suggesting these spectroscopic properties are directly related and that compounds responsible for UV-Vis absorbance are also responsible for fluorescence. Preliminary data suggest that DOM plays a central role in trace metal speciation in atmospheric waters where complexation influences the photochemical properties of the DOM as well as the photochemically mediated cycling of the metals. DOM is the dominant complexing agent for iron increasing the stability of Fe (II) and thus the solubility of iron in both rainwater and seawater. Given the probability of multiple sources for rainwater DOM, with correspondingly different compositional signatures, we will also evaluate its chemical characteristics. Humic-like substances, substances that have been shown as important chromophores in surface waters, can be derived from different sources and are notoriously ill-defined (Diallo et al. 2003), but offer

the most probable source of chromophoric DOM in rainwater (Capiello et al. 2003). Humic substances may be incorporated into precipitation from wind blown soil particles or formed in the atmosphere from oxidation of soot (Decesari et al. 2002).

In addition to quantifying how much DOM is present in rainwater; it would be extremely useful to begin to evaluate its chemical characteristics. The chemical character of DOM in rainwater reflects its mixed origin and will be examined by UV-Vis, excitation emission spectroscopy (EEMs), and nuclear magnetic resonance (NMR). While the absorption coefficient at 300nm has been used as an index of DOM abundance (Castillo et al. 1999), spectral slopes calculated from log linear least-square regressions of absorption coefficients versus wavelength could convey information about the molecular weight of DOM. Excitation and emission spectra can be employed to discriminate between DOM types and to gain insight into the structural nature of the chromophores of the rainwater (Blough et al. 1995). Finally, ^{1}H NMR was used for analyzing the structure of macromolecular compounds (Suzuki et al. 2001). Complex signals (broad or sharp lines) can be examined and characteristics such as aromatic absorbance and aliphatic nature can be determined.

In summary, the goals of this thesis are two-fold. 1) Quantify DOM UV-Vis absorbance and fluorescence in authentic and fractionated rainwater samples collected during different seasons and different storm types. 2) Evaluate structural characteristics of rainwater DOM.

EXPERIMENTAL

Rainwater/Sampling

Rainwater was collected on the UNCW campus on an event basis throughout the time period of September 15, 2005 to September 6, 2006. The UNCW rainwater collection site is a large open area, approximately one-hectare, within a turkey oak, long leaf pine, and wire grass

community, typical of inland coastal areas in southeastern North Carolina. This rainwater site (34°13.9'N, 77°52.7'W) is on the UNCW campus, approximately 8.5 km from the Atlantic Ocean. There are over 15 years of rainwater composition data for this site, which will be useful in interpretation of the data generated and also will allow comparison with other locations. Because of the proximity of the sampling location to the laboratory, dissolved organic matter (DOM) analyses can be initiated within minutes of collection, which reduces the possibility of compositional changes between the time of collection and analysis.

Four Aerochem-Metrics (ACM) Model 301 Automatic Sensing Wet/Dry Precipitation Collectors were used to collect event rain samples. One of these ACM containing a 4L muffled Pyrex glass beaker from which samples for pH, inorganic ions, dissolved organic carbon, hydrogen peroxide, organic acids and DOM were collected and analyzed. The remaining three ACM were used for trace metal sample collection. These consisted of a high density polyethylene (HDPE) funnel connected by Tygon® FEP- lined tubing to a 2.2L Teflon bottle, all cleaned using trace metal clean procedures and protocols (Bruland et al., 1979; Bruland, 1980). Meteorological data including rain amounts, rain duration, time of day, surface temperature, wind speed, wind direction and storm origin were also recorded. Rain events were characterized by E# where E represents rain event and # corresponds to a specific rain event number. Real time precipitation maps were used to define the end of specific rain events, which initiated the sampling process.

Trajectories

Air mass, 72 hour back trajectories were used to classify each individual rain event. The two trajectories used in this study were terrestrial and marine. Each trajectory is compromised of three regions of different heights above sea level. The terrestrial storm is deemed as such if each

of the three air masses derived over land. The marine storm is deemed as such if the three air masses derive over the sea.

Reagents and Standards

All chemicals were reagent grade or HPLC grade unless stated otherwise. A Milli-Q Plus Ultra-pure water system (Millipore, Bedford, MA) provided water (>18MΩ) for all analysis, dilutions, reagent and standard preparations. Internal NMR stock primary standard was prepared by adding 10 mg of 3-(Trimethylsilyl)propionic-2,2,3,3-d_4 acid (98.0%), sodium salt to 1.0mL Deuterium oxide (99.96%, D_2O). The primary stock standard (0.01M) was diluted by a factor of ten and 20 µL was added to the sample in D_2O (0.60mL) giving a final TMS concentration of 187 µM in each sample.

Hydrophobic DOM Extraction

Hydrophobic dissolved organic matter, operationally defined here as C_{18} extractable dissolved organic matter (DOM) substances, were extracted using C_{18} cartridges (Waters Chromatography, Milford, MA) by the method of Amador et al. (1990). This technique was chosen over conventional methods using XAD resins because in surface waters it has been demonstrated that the C_{18} is efficient at removing the fluorescent DOM. Amador et al. (1990) reported that C_{18} extraction of humic substances from seawater was between 22 and 84% more effective relative to XAD-2. Kuo et al. (1993) also recovered 83% of an aquatic fulvic acid using C_{18} solid-phase extraction. In addition, Amador et al. (1990) found C_{18} extraction better able to retain the UV-visible and fluorescence characteristics of the isolated humic material relative to XAD. Since these were the characteristics of most interest in this study, C_{18} extraction was the most logical choice of an extraction procedure. A second advantage of using C_{18} extraction is that 90% methanol/ 10% water is the eluant rather than 0.1M NaOH. Therefore,

any degradation of DOC due to high pH is avoided.

Samples were warmed to room temperature and filtered through 0.2μm, acid-washed Gelman Supor® polysulfonone filters enclosed in a muffled glass filtration apparatus. C_{18} cartridges were preconditioned by washing with 2 X 5 mL 90% methanol/ 10% water followed by 2 X 5 mL deionized water. Filtered rainwater was extracted by passing 50 mL, unless otherwise noted, through the C_{18} cartridge. The cartridges were washed with 2 X 5 mL of deionized water to remove residual salts and DOM was eluted with 6 mL of 90%/ methanol 10% water solution. Samples were pulled through C_{18} cartridges by the house vacuum and collected in a 500 mL side-arm flask. Samples were eluted into 25mL muffled round-bottom flasks and concentrated to dryness under reduced pressure (Buchi Rotavapor, Model RE 111, Switzerland). Traces of water were removed under vacuum (Sargent-Welch Model 1400, Skokie, IL). The eluted sample was then reconstituted into DI water and sonicated for 30 seconds. Aliquots from the whole rainwater sample, what was retained on the cartridge, and what was not retained on the cartridge were analyzed.

Terminology

Each rain event was extracted by the C_{18} cartridge resulting in three fractions being collected. The fraction which was not passed through the C_{18} cartridge is termed the whole sample. The fraction that was extracted, eluted, and reconstituted was termed the reconstituted sample. The fraction that passed through the cartridge was termed filtrate.

UV-Vis Absorption Spectroscopy

Absorption spectra was obtained between 240 and 800 nm at 1 nm intervals using a double-beam spectrophotometer equipped with matching 10 cm quartz cells. Each sample was scanned four times, and the resulting spectra was smoothed and averaged. The data was

corrected for scattering and baseline fluctuations by subtracting from each spectrum the value of absorption at 700 nm (Del Castillo et al. 1999).

The absorption coefficients (a) were calculated from the absorbencies using:

$$a\ (\lambda) = 2.303A(\lambda) / r$$

where A is the absorbance (Log I_o / I) and r is the pathlength in meters. The absorption coefficient at 300 nm were used as an index of colored dissolved organic matter (DOM) abundance. The spectral slopes were calculated from linear least-square regressions of the plot of ln $a(\lambda)$ vs. wavelength for the interval between 270 and 350 nm and were used as a proxy for molecular weight ranges. The spectral slope will decrease with increasing molecular weight.

Excitation emission spectroscopy

Excitation-emission matrix (EEM) fluorescence properties are determined on a Jobin Yvon SPEX Fluoromax-3 scanning fluorometer equipped with a 150 W Xe arc lamp and a R928P detector. Although higher resolution is possible, EEMS are generally constructed by using excitation wavelengths from 250 to 500nm (4 nm intervals) and scanning emission from 280 to 550nm (4 nm intervals). The instrument is configured to collect the signal in ratio mode with dark offset using 5nm bandpasses on both the excitation and emission monochromators. The EEMs were created by concatenating emission spectra measured every 5nm from 250 to 500nm at 51 separate excitation wavelengths (Del Castillo et al. 1999). Scans are corrected for instrument configuration using factory supplied correction factors, which are determined essentially as described in Method 1 of (Coble et al. 1993). Post processing of scans is performed using FLToolbox 1.91 developed by Wade Sheldon (University of Georgia) for MATLAB® (Release 11). The software eliminates Rayleigh and Raman scattering peaks by excising portions (± 10-15 nm FW) of each scan centered on the respective scatter peak. The

excised data is replaced using three-dimensional interpolation of the remaining data according to the Delaunay triangulation method and constraining the interpolation such that all nonexcised data is retained. Following removal of scatter peaks, data were normalized to a daily-determined water Raman intensity (275ex / 303em, 5 nm bandpasses) and converted to Raman normalized quinine sulfate equivalents (QSE) in ppb (Coble et al. 1998). An average of 4 Milli-Q water blank extractions were subtracted to eliminate the water-Raman peaks. Optical aberrations produces by spectral biases from all the optical components of the instrument were corrected. Replicate scans are generally within 5% agreement in terms of intensity and within bandpass resolution in terms of peak location. Peak locations are labeled as defined in (Coble 1996).

Nuclear Magnetic Resonance (NMR)

Liquid phase ^{1}H-NMR were recorded on a Bruker Avance 400 MHz NMR spectrometer. The DOM that was extracted for NMR analysis was done in the same fashion as previously described with the exception of adding 0.60mL of D_2O and an internal standard (20 µL of 3-(Trimethylsilyl) propionic-2,2,3,3-d_4 acid (98.0%), sodium salt) to the completely dried DOM extract remaining in the 25mL round-bottom flask. The solution was swirled around the flask and sonicated; the mixture was removed with a 5cc syringe (Popper & Sons, NY), and placed into a 5mm NMR tube. The sample was placed in a sonicator for 5 seconds to assure the internal standard was mixed well with the sample.

An initial ^{1}H proton experiment (zg30, 64 scans) (Werner 1994) was used to find the resonance of the HDO peak which is a result of exchange of O-H and N-H protons in the sample with the D_2O solvent. Due to the large HDO peak, presaturation techniques (power level 20 dB) were used to help eliminate phasing and integration problem. Each sample was then analyzed using a presaturation experiment (zgpr, 1024 scans) where: pulse angle = 30º (P1 = 9.00 µsec),

D1 = 3.00 sec, and PL = 60 dB. The probe used was an inverse gradient probe. After the acquisition, the FID was transformed with exponential multiplication (LB = 5). Line Broadening (LB) is a mathematical manipulation of the data that enhances small signals, which may be otherwise lost in the baseline noise. Phasing, calibration, and integration were done identically for all experiments to allow for comparisons of different rain events. After phasing, the standard was set to zero ppm.

The following regions were integrated: 9.0 to 6.5 ppm, 4.5 to 3.4 ppm, 3.3 to 1.9 ppm, 1.9 to 1.1 ppm, 1.1 to 0.5 ppm, and 0.1 to –0.1 ppm (internal standard) were made to allow for comparison of different natures of extracted DOM. The 10 to 9.5 ppm and 6.5 to 6.0 ppm regions were also integrated to correct for baseline anomalies and drift. The internal standard was calibrated to zero and integrated to one. The two regions that were used to correct for baseline drift were subtracted from the integration of the respected region after being multiplied by the area of the region. Total abundance of the respective regions were then calculated as well as a percentage of the entire regions.

Dissolved Organic Carbon (DOC)

The whole rainwater and the reconstituted fraction were analyzed for its DOC and TDN content. The filtrate was not analyzed for DOC concentration due to the residual methanol that was present in the sample causing an inaccurate measurement. Rain samples were analyzed for DOC by high temperature combustion (HTC) using a Shimadzu TOC 5000 total organic carbon analyzer equipped with an ASI 5000 autosampler as described in (Willey et al. 2000). A primary standard was prepared from 215 mg potassium hydrogen phthalate (KHP) dissolved in 100mL of Milli-Q water. A secondary KHP solution was prepared monthly and consisted of ~25g of the KHP primary solution diluted gravimetrically to 250mL with Milli-Q water. Standards in the

range of 33 – 400 μM C were made weekly from the secondary KHP stock solution.

The samples were injected (75 μL) into the Shimadzu TOC-5050A furnace, filled with a preconditioned Shimadzu catalyst (Al_2O_3 impregnated with 0.5% platinum), at 680ºC. The combustion products (CO_2, NO•, H_2O, etc.) are carried by high purity CO_2 free air through an in-built Peltier cooler at ~1ºC (electronic dehumidifier) for removal of water vapor followed by a Shimadzu particle filter (20 mm, sub-micron membrane) and finally into the Shimadzu detector cell.

RESULTS AND DISCUSSION

Volume Study to Determine $_{C18}$ Extraction Efficiency

A study was conducted on rain event 620 to determine how extraction volume influences the total recovery of rainwater fluorescent DOC. Total recovery was determined from the sum of fluorescence in the reconstituted and filtrate fractions on the C_{18} cartridge relative to the fluorescence of the whole rain. The study involved extracting several volumes (50, 100, 200, and 500 mL) of the same rain and determining the fluorescence on the three fractions. An extraction volume of 50 mL resulted in the greatest total recovery (~70%) of DOM fluorescence (Figure 1). As the extraction volume increased, the total recovery of DOM fluorescence decreased. The fraction of DOM fluorescence in the filtrate did not vary substantially with extraction volume, suggesting that the relative amount of DOM bound to the C_{18} cartridge did not change with increasing sample volume. Rather the decrease in total recovery and the percent reconstituted on the C_{18} cartridge with increasing volume can be explained by an inefficient elution of DOM from the C_{18} cartridge at high extraction volumes. Based on these results, an extraction volume of 50 mL was used for all rain events during this study.

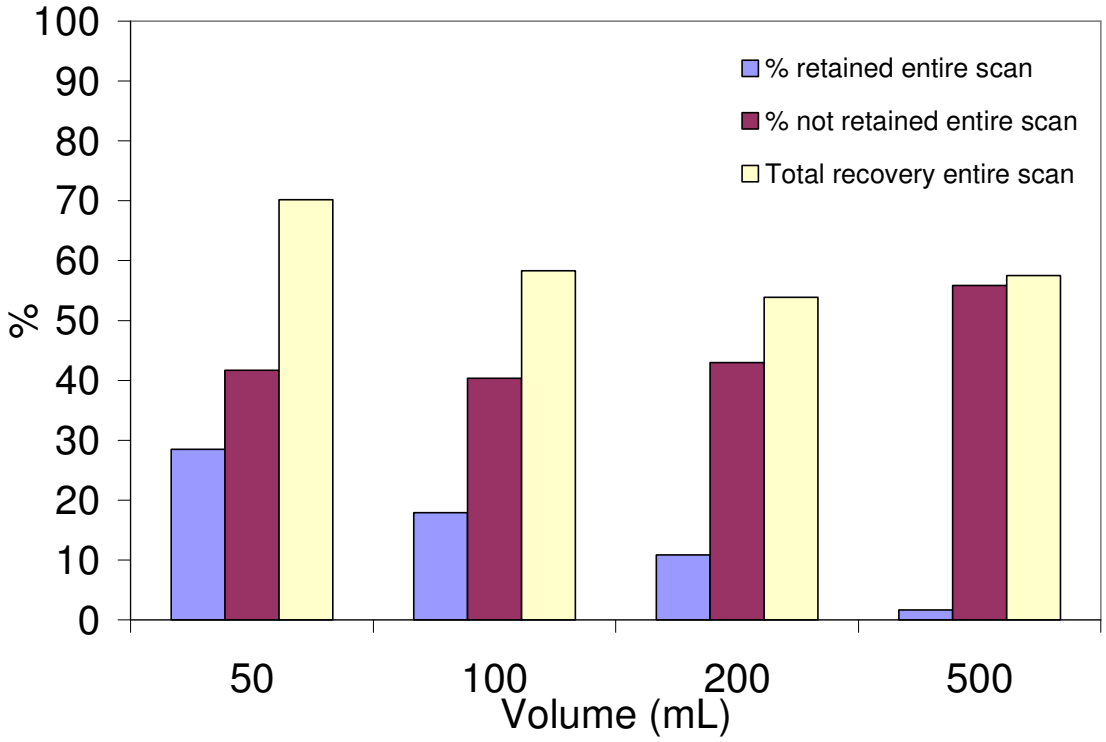

Figure 1. Percent reconstituted DOM fluorescence, percent filtrate, and total recovery as a function of rainwater extracted. The percent fluorescence is based on the integration of the entire EEMs scan.

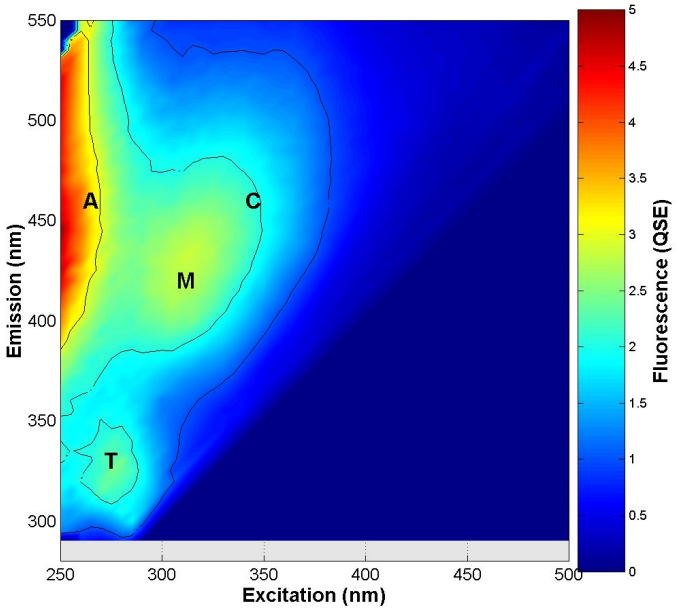

Figure 2. Typical EEM spectra of rain event 417. The A, M, C, and T labels are based upon Coble (1996), where A and C indicate terrestrial humic-like substances, M is marine humic-like material and T indicates the presence of protein-like substances. Regions used for integration for the A, C, M, and T peaks respectively were Ex 220-275 nm, Em 357-563 nm; Ex 320-370 nm, Em 435-485 nm; Ex 287-337 nm, Em 395-445nm; Ex 250-300 nm, Em 305-355nm.

Absorbance and Fluorescence

Excitation Emission Spectroscopy (EEMS) spectra were integrated and volume weighted averages (VWA) determined for the entire scan (scatter reducing) (Table 1a). A typical EEM of rain event 417 is presented in figure 2. The fluorescences ranged from 21.8 to 215 x 10^{-3} (Table 1b) while the VWA fluorescence of the whole sample was 57,700 (Table 1a). The absorbances ranged from 0.175 to 2.86 m-1 (Table 2a) while the VWA absorbance at 300 nm was 0.67 m^{-1} (Table 2b). Both these values are somewhat higher than previously reported for rain collected at this same site (29,000 and 0.37 m^{-1} respectively) between February 21, 2002 and August 11, 2003 (Kieber et al., 2006). Since the DOC concentration in this study are similar, this suggests that the rain analyzed during this study has higher chromophoric properties than previously collected rainwater samples.

The average spectral slopes, calculated from UV-Vis absorption spectra of whole and reconstituted rain, were 23.5 μm^{-1} and 10.3 μm^{-1} respectively (Table 2b). The spectral slopes ranged from 7.19 μm^{-1} to 45.5μm^{-1} and 6.22 μm^{-1} to 17.8 μm^{-1} respectively (Table 2a). Previous work has suggested an inverse relationship of surface water DOC molecular weight with spectral slope coefficient (De Haan, 1993; Strome and Miller, 1978) where a higher spectral slope is indicative of lower molecular weight material. Based on the properties of the C_{18} cartridge, the DOM reconstituted off the C_{18} cartridge is hydrophobic while the filtrate fraction is relatively more hydrophilic. The material retained by the C_{18} cartridge is likely the high molecular weight compounds. Therefore, the smaller spectral slope of the retained fraction relative to the whole sample agrees with previous work.

Table 1a. Volume weighted average from the fluorescent integration entire scan (scatter reducing) peak maxima. Percent integrated fluorescence retained, filtrate, and total recovery (relative to entire scan). All data is represented with +/- one standard deviation. n = number of samples and amt = rain amount in mm.

	n	Amt. (mm)	Integrated Fluorescence whole x 10^{-3}	% Integrated Fluorescence reconstituted	% Integrated Fluorescence filtrate	% Integrated Fluorescence Total recovery
All Data	37	561	57.7 +/- 7.46	26.7 +/- 11.7	52.1 +/- 14.6	78.8 +/- 17.8
All Warm	30	430	62.6 +/- 8.98	27.1 +/- 12.1	53.5 +/- 15.6	80.7 +/- 18.6
All Cold	7	131	41.7 +/-8.69	24.7 +/- 10.8	46.4 +/- 7.50	71.2 +/- 13.9
Terrestrial	15	216	49.8 +/-9.08	26.8 +/- 12.7	49.1 +/- 8.85	75.9 +/- 15.5
Marine	4	33.0	50.1 +/-6.36	38.8 +/- 16.3	49.3 +/- 6.83	88.1 +/- 24.9

Table 1b. Ranges of volume weighted average from the fluorescent integration entire scan (scatter reducing) peak maxima. Ranges of percent integrated fluorescence retained, filtrate, and total recovery (relative to entire scan) n = number of samples and amt = rain amount in mm.

	N	Amt. (mm)	Integrated Fluorescence whole x 10^{-3}	% Integrated Fluorescence reconstituted	% Integrated Fluorescence filtrate	% Integrated Fluorescence Total recovery
All Data	37	561	21.8-215	9.97-53.8	32.5-107	42.5-161
All Warm	30	430	32.7-113	9.97-53.8	32.5-107	42.5-161
All Cold	7	131	21.8-215	11.3-39.0	38.9-58.1	50.2-97.1
Terrestrial	15	216	24.0-161	9.97-49.4	33.8-58.1	43.8-108
Marine	4	33.0	32.4-62.9	15.7-53.9	43.4-56.8	59.1-111

Table 2a. Ranges of volume weighted average of absorbance at 300 nm. Ranges of percent absorbance retained, filtrate, and total recovery are represented as well as spectral slope coefficients of whole and reconstituted portions at 300 nm.
n = number of samples and amt = rain amount in mm.

	n	Amt. (mm)	Abs @ 300 nm whole (m^{-1})	Abs @ 300 nm (m^{-1}) % reconstituted	Abs @ 300 nm (m^{-1}) % filtrate	Abs @ 300 nm (m^{-1}) % total recovery	Spectral slope coefficient whole(μm^{-1})	Spectral slope coefficient reconstituted (μm^{-1})
All Data	32	492	0.175-2.86	23.6-420	20.0-119	43.6-539	7.19-45.5	6.22-17.8
All Warm	28	403	0.175-2.86	23.6-420	23.2-119	46.8-539	7.19-45.5	6.22-17.8
All Cold	4	88.1	0.276-1.08	28.8-89.1	20.0-88.6	48.8-178	15.8-20.1	7.87-11.1
Terrestrial	14	211	0.175-2.86	23.6-350	20.0-88.6	43.6-439	16.9-45.5	6.27-17.8
Marine	4	33.0	0.250-0.598	73.8-218	26.8-43.0	100-261	7.19-37.9	7.89-12.7

Table 2b. Volume weighted average of absorbance at 300 nm. Percent absorbance retained, filtrate, and total recovery are represented as well as spectral slope coefficients of whole and reconstituted portions at 300 nm. All data is represented with +/- one standard deviation. n = number of samples and amt = rain amount in mm.

	n	Amt. (mm)	Abs @ 300 nm whole (m^{-1})	Abs @ 300 nm (m^{-1}) % reconstituted	Abs @ 300 nm (m^{-1}) % filtrate	Abs @ 300 nm (m^{-1}) % total recovery	Spectral slope coefficient whole(μm^{-1})	Spectral slope coefficient reconstituted (μm^{-1})
All Data	32	492	0.67 +/- 0.11	116 +/- 99.0	43.1 +/- 20.4	156 +/- 101	23.5 +/- 7.17	10.3 +/- 2.96
All Warm	28	403	0.72 +/- 0.12	124 +/- 103	41.3 +/- 17.7	165 +/- 105	24.1 +/- 7.64	10.8 +/- 3.05
All Cold	4	88.1	0.44 +/- 0.11	60.7 +/- 25.4	55.3 +/- 34.8	100 +/- 32.2	17.6 +/- 2.20	9.40 +/- 1.37
Terrestrial	14	211	0.59 +/- 0.16	121 +/- 110	43.6 +/- 20.7	157 +/- 114	23.5 +/- 7.37	10.9 +/- 3.49
Marine	4	33.0	0.45 +/- 0.068	149 +/- 65.8	36.9 +/- 8.80	185 +/- 75.0	23.5 +/- 13.4	9.48 +/- 2.19

Based on the fluorescence of the reconstituted and filtrate fractions relative to the fluorescence of the whole samples, 79% of the DOM fluorescence was accounted for in the two fractions (Table 1a), ranging from 42.5 to 161 % (Table 1b). Of the recovered DOM fluorescence, 52% is from relatively more hydrophilic entities, ranging from 32.5 to 107%, because they were not retained by the hydrophobic C_{18} cartridge. The fluorescent DOM in the reconstituted fraction, 27% of the recovered DOM fluorescence, ranging from 9.97 to 53.8%, is from more hydrophobic compounds. The fraction of unrecovered DOM fluorescence most likely a results from inefficient elution off the C_{18} cartridge of very hydrophobic or strongly bound material.

The results presented in Table 2b and 1a are different than similar studies done in surface waters. Approximately 70% of DOM from surface waters was effectively removed by C_{18} cartridge extraction which is larger than the percentage from rainwater (Amador et al. 1989). DOM has been proposed to consist primarily of humic-like substances which would be efficiently retained by the C_{18} cartridge (Cappiello et al., 2003). However, since 52% of the rainwater fluorescent material was not retained by the C_{18} cartridge, this suggests rainwater DOM contains chromophoric molecules that are different than surface waters and probably contain a larger fraction of small, nonpolar molecules.

The UV-Vis absorbance percentages were also calculated in the same fashion as the fluorescence, but since the total recoveries were greater than 100% (ranges of 81.4 to 539%) it appears that a contamination was present (Table 2b). Previous work on whole rainwater showed a positive correlation between fluorescence and absorbance (Kieber et al. 2006). The absorbance and fluorescence of whole rainwater measured in my study fall within the range of previously reported absorbance and fluorescence values indicating the contamination was likely picked up

during the extraction procedure. The reported absorbances include the subtraction of the absorbance from blank extractions, determined by passing milli-Q water through clean C_{18} cartridges. Therefore, the contamination in the sample is in addition to the absorbances associated with these blanks.

Dissolved Organic Carbon

Dissolved organic carbon analysis was performed on a subset of rainwater samples. The VWA absorbance (Table 3a) and fluorescence (Table 3b) of the whole rain, along with the percent of fluorescence reconstituted, filtrate, and total recovery in this subset of samples is similar to the values obtained using the whole data set. Tables 4a and 4b include the respective ranges for the fluorescence and absorbance. This indicates that the DOC sample subset provides a representative fraction of the whole data set. The VWA DOC concentration was 62 µM, ranging from 29.6 to 599µM, which is similar to the previously reported value of 61 µM for rainwater collected at the same site (Kieber et al. 2006). The C_{18} reconstituted fraction of the rainwater accounted for 42%, ranging from 12.8 to 126%, of the DOC from the rain sample. This suggests that C_{18} reconstituted DOC is a significant fraction of the uncharacterized DOC in rainwater. The total recovery of DOC could not be determined since the filtrate was contaminated with residual methanol. The 42% should be viewed as a minimum estimate as some fraction of the DOC most likely was retained and not eluted off the C_{18} cartridge based on the approximate 20% of the DOC fluorescence not recovered from the C_{18} cartridge. For surface water samples, the percentage of DOC extracted by C_{18} cartridges were less than the percentage of chromophoric material retained (based on fluorescence or UV absorbance) (Simjouw et al., 2005; Kim et al., 2003). The reverse was found with rainwater, providing further evidence that the chromophoric DOC in rainwater is different from surface water DOM. Previously, the

portion of characterized DOC in rain consisted of organic acids (Kieber et al. 2006), compounds which would be expected to be present in the filtrate portion of the extracted rain. Therefore, the 42% of DOC found in the reconstituted fraction consists of organic matter which has not previously been characterized in rainwater.

Table 3a. DOC subset of volume weighted average of absorbance at 300 nm. Percent absorbance retained, filtrate, and total recovery are represented as well as spectral slope coefficients at 300 nm. All data is represented with +/- one standard deviation. n = number of samples and amt = rain amount in mm.

DOC subset	n	Amt. (mm)	Abs @ 300 nm whole (m^{-1})	Abs @ 300 nm (m^{-1}) % reconstituted	Abs @ 300 nm (m^{-1}) % filtrate	Abs @ 300 nm (m^{-1}) % total recovery	Spectral slope coefficient whole(μm^{-1})	Spectral slope coefficient reconstituted (μm^{-1})
All Data	17	237	0.70 +/- 0.24	134 +/- 125	37.9 +/- 8.79	173 +/- 131	24.3 +/- 8.65	9.82 +/- 2.75
All Warm	15	193	0.76 +/- 0.27	146 +/- 128	39.0 +/- 7.60	185 +/- 133	25.3 +/- 8.69	10.0 +/- 2.87
All Cold	2	44.0	0.46 +/- 0.33	42.2 +/- 18.9	25.5 +/- 7.84	67.7 +/- 26.8	16.4 +/- 0.757	8.35 +/- 0.680
Terrestrial	10	153	0.59 +/- 0.14	143 +/- 125	37.0 +/- 11.1	180 +/- 132	24.1 +/- 8.32	9.97 +/- 3.22
Marine	2	16.0	0.41 +/- 0.10	95.5 +/- 30.6	41.0 +/- 10.2	136 +/- 40	28.2 +/- 13.6	10.5 +/-3.07

Table 3b. DOC subset of volume weighted average DOC and integrated fluorescence. Percent DOC retained and percent integrated fluorescence retained, filtrate, and total recovery (relative to entire scan). All data is represented with +/- one standard deviation. n = number of samples and amt = rain amount in mm.

DOC subset	n	Amt. (mm)	DOC whole (µM)	% DOC reconstituted	Integrated Fluorescence whole x 10^{-3}	% Integrated Fluorescence reconstituted	% Integrated Fluorescence filtrate	% Integrated Fluorescence Total recovery
All Data	18	260	62.3 +/- 4.45	41.6 +/- 28.69	54.7 +/- 10.6	24.02 +/- 11.71	49.76 +/- 10.44	73.78 +/- 17.74
All Warm	15	193	137 +/- 28.59	35.1 +/- 19.27	62.0 +/- 13.02	25.12 +/- 12.54	51.54 +/- 10.85	76.66 +/- 18.58
All Cold	3	67.0	39.5 +/- 4.43	74.6 +/- 49.46	33.8 +/- 5.69	18.52 +/- 3.46	41.41 +/- 2.80	59.93 +/- 6.18
Terrestrial	10	153	111 +/- 23.36	30.5 +/- 18.34	41.8 +/- 8.52	24.3 +/- 13.71	50.35 +/- 9.31	74.65 +/- 18.03
Marine	2	16.0	59.6 +/- 3.03	38.1 +/- 13.56	44.0 +/- 10.09	28.85 +/- 18.60	56.79 +/- 6.83	85.64 +/- 21.55

Table 4a. Ranges for DOC subset of volume weighted average DOC and integrated fluorescence. Ranges of percent DOC retained and percent integrated fluorescence retained, filtrate, and total recovery (relative to entire scan). n = number of samples and amt = rain amount in mm.

DOC subset	n	Amt. (mm)	DOC whole (µM)	% DOC reconstituted	Integrated Fluorescence whole x 10^{-3}	% Integrated Fluorescence reconstituted	% Integrated Fluorescence filtrate	% Integrated Fluorescence Total recovery
All Data	18	260	29.6-599	12.8-126	24.0-215	9.97-49.4	32.5-69.9	42.5-119
All Warm	15	193	47.1-599	12.8-75.7	24.0-215	9.97-49.4	32.5-69.9	42.5-119
All Cold	3	67.0	29.6-49.4	26.8-126	32.7-34.9	14.8-21.6	38.9-44.5	53.7-66.1
Terrestrial	10	153	42.0-326	12.8-71.5	24.0-161	9.97-49.4	33.8-67.8	43.8-117
Marine	2	16.0	56.1-64.9	28.5-47.7	56.1-64.9	15.7-42.0	46.9-67.0	62.6-109

Table 4b. Ranges for DOC subset of volume weighted average of absorbance at 300 nm. Ranges of percent absorbance retained, filtrate, and total recovery are represented as well as spectral slope coefficients at 300 nm. n = number of samples and amt = rain amount in mm.

DOC subset	n	Amt. (mm)	Abs @ 300 nm whole (m^{-1})	Abs @ 300 nm (m^{-1}) % reconstituted	Abs @ 300 nm (m^{-1}) % filtrate	Abs @ 300 nm (m^{-1}) % total recovery	Spectral slope coefficient whole(μm^{-1})	Spectral slope coefficient reconstituted (μm^{-1})
All Data	17	237	0.170-2.46	23.0-420	20.0-55.6	43.0-475	14.4-45.5	6.42-16.3
All Warm	15	193	0.170-2.46	23.0-420	28.8-55.2	51.8-475	14.4-45.5	6.42-16.3
All Cold	2	44.0	0.403-0.564	28.7-55.6	20.0-31.1	48.7-150	15.87-16.9	7.87-8.83
Terrestrial	10	153	0.170-2.33	23.7-350	20.0-55.6	43.6-405	16.9-45.5	6.27-12.79
Marine	2	16.0	0.256-0.598	73.8-117	31-51	105-168	18.7-37.9	8.35-12.8

Nuclear Magnetic Resonance (NMR)

NMR spectroscopy is a powerful tool for the determination of functional groups in DOM. The nuclear magnetic resonance spectra that are obtained for pure organic compounds in solution generally consist of very sharp, well-defined lines (Aiken et al. 1985). The extreme sharpness of these lines allows one to detect very small differences in the magnetic environments of nuclei. However, DOM mixtures are complex and result with broader peaks.

Comparisons of ^{1}H-NMR integral areas allows for comparison of different chemical natures of DOM. The relative regions of this study are identified by five most representative categories of functional groups in the ^{1}H-NMR spectra: Ar-H: aromatic protons (9-6.5 ppm), CH-O: protons on carbon atoms singly bound to oxygen atoms (4.5-3.3 ppm), CH-C=: aliphatic protons on carbon atoms adjacent to carbonyl groups or aromatic rings (3.2-1.9 ppm), CH_2- groups (1.9-1.1 ppm), and CH_3- groups (1.1-0.5 ppm). Comparison of the total NMR integration as well as integrals of the individual regions allows for comparisons of abundances of different protons in different rain samples.

As shown in the NMR spectra of two different rain events (Figure 3 a and b), the most intense bands can be seen within the region of 4.5 to 0.8 ppm which includes the CH-O, CH-C=, CH_2 and CH_3 groups. On occasion, bands in the aromatic region of 9.0 to 6.5 ppm can be observed. The terrestrial originated storm had a higher total integration (Figure 4a) as well as a higher percentage of CH-O protons than the marine originated storm (Figure 4b), while the blank reveals very low integration and intensity in all regions (Figures 3c and 4a).

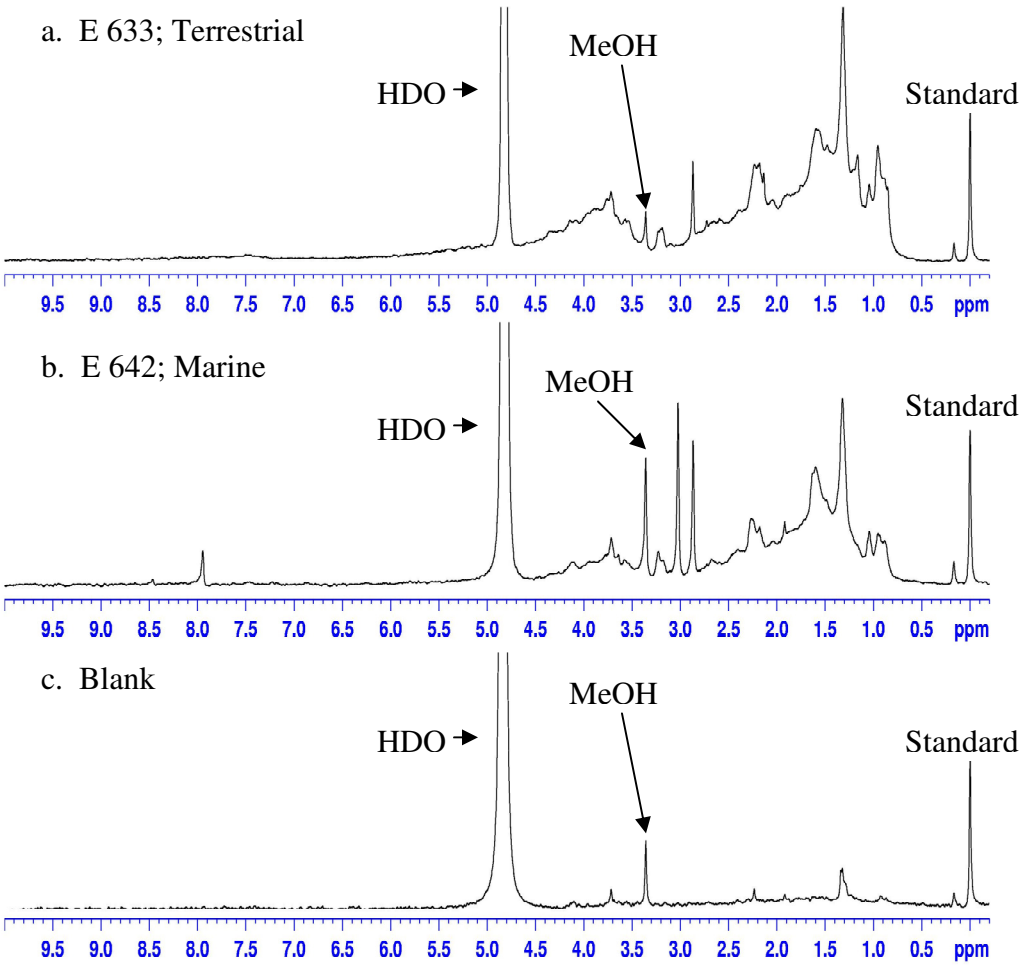

Figure 3. NMR spectra of (a) rain event 633, terrestrial; (b) rain event 642, marine; and (c) blank.

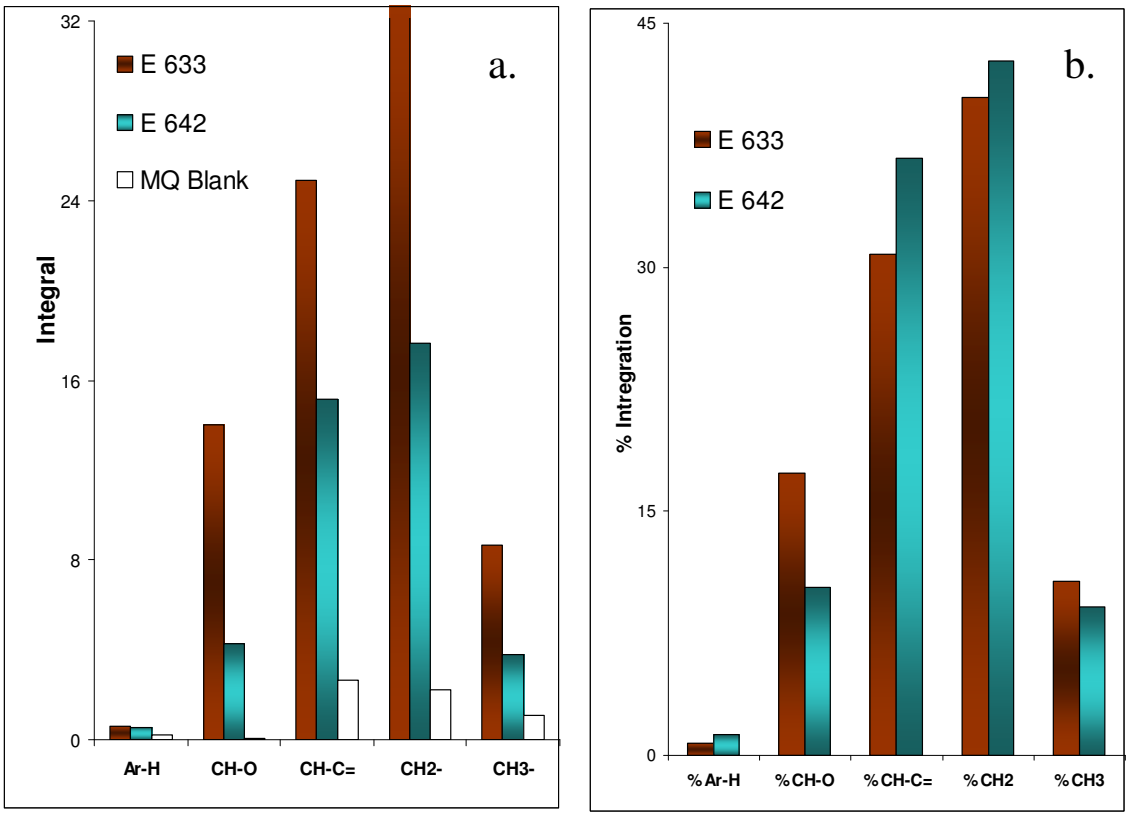

Figure 4 (a) Average of respective NMR integrated regions and (b) % integration of respective regions for marine (E642) and terrestrial (E633) originated storms.

In order to assess whether the NMR differences between rain events are not due to variability in the method, a variability study of rain event E 658 was conducted on 4 aliquots. Average total integrations as well as the average integrations in the respective regions were determined (Table5).

Table 5. Variability study: standard deviations, relative standard deviations, and averages of NMR integral regions of E 658.

	Ar-H	CH-O	CH-C=	CH2-	CH3-
Average Integration	0.359	3.03	4.98	7.51	2.15
Relative% Standard Deviation	27.3	8.24	3.53	8.82	4.63
Standard deviation	0.0983	0.250	0.176	0.663	0.100

The relative standard deviation was 27.3% for the Ar-H region, which is large in comparison to the other regions. This is due to the average integration value being small.

However, the Ar-H region shows the smallest standard deviation (Figure 5). The largest standard deviation is from the CH_2- region. All other relative standard deviations were less than 9% indicating low variability from the extraction and NMR methods.

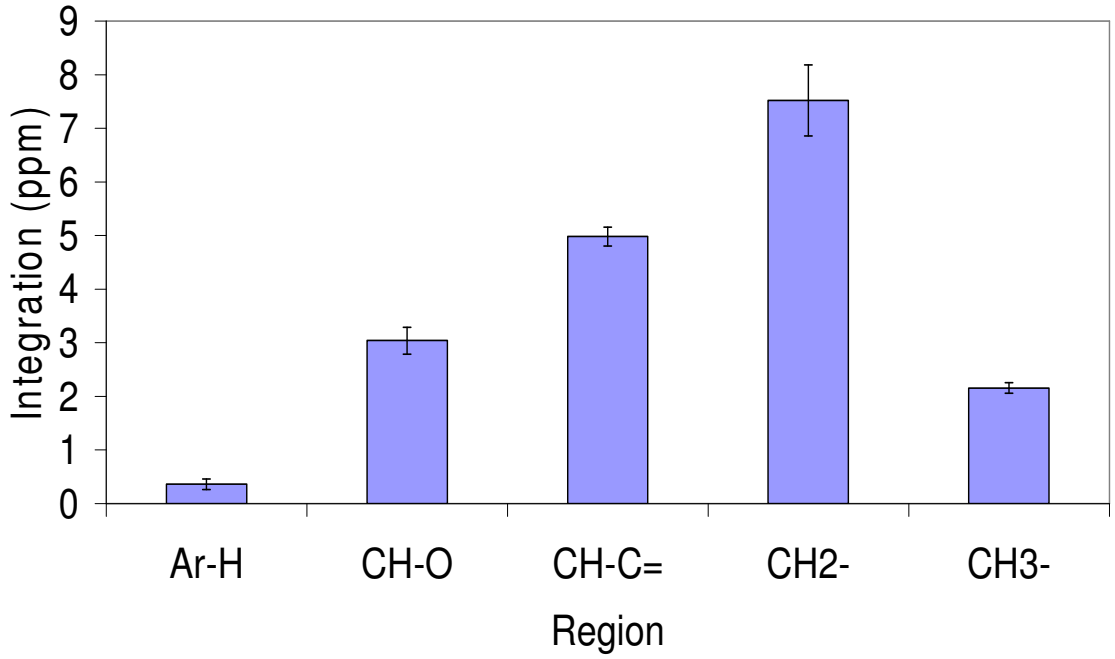

Figure 5. Average NMR integrated regions of 4 samples of rain event 658 with respective standard deviations per integrated area.

Fluorescence total integration from the whole (Figure 6) and reconstituted fraction values of 36 rain events were plotted against the total NMR integration. Whole and reconstituted fluorescence total integration values were also plotted against each individual NMR integral area.

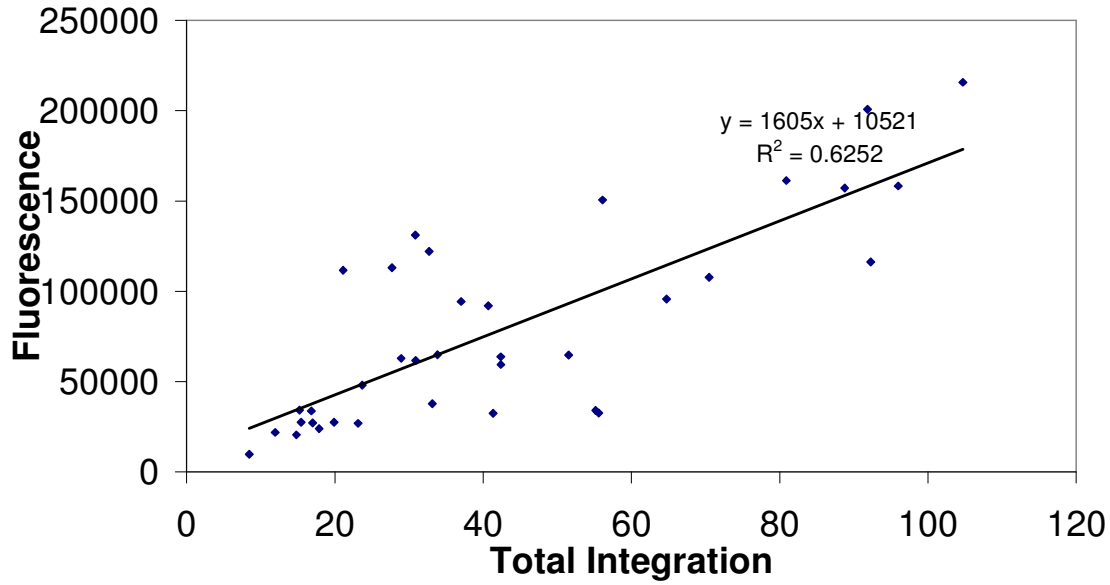

Figure 6. Whole fluorescence vs. total NMR integration of all rain samples.

Tables 6 through 9 show the slopes, R values, and P values resulting from each plot of whole and reconstituted total fluorescence integration values *vs* NMR integrals. A strong correlation exists between the total ($P < 0.001$) and individual integrated NMR regions and both the whole and reconstituted fluorescence (Table 6). Comparing the slopes of the fluorescence vs the integral values of individual NMR regions (Δ Fluorescence/ Δ NMR integration), the greatest contributor to the fluorescence is the Ar-H region (Table 6). Thus, although the Ar-H region is the smallest contributor to the total NMR integration (Figure 5), it is the largest contributor to the fluorescence, suggesting that the Ar-H region is responsible for most of the fluorescence.

Total NMR integration values, as well as each individual NMR integral areas, were also plotted against the whole and reconstituted DOC values. Strong correlations exist between the total ($P < 0.001$) and individual integrated NMR regions and both whole and reconstituted DOC values (Table 7). Comparing the slopes of the integrals of individual NMR regions vs DOC (ΔNMR integration/ΔDOC), the NMR regions showing the greatest increase with increasing

DOC are the CH-C= and CH_2 hydrogens. The region which contributes least to the DOC is the aromatic region (Table 7).

Tables 10 and 11 show the slopes, R values, and P values resulting from each plot of whole and reconstituted total fluorescence integration values of each respective peak (A, C, M, and T) *vs* NMR integrals. A correlation exists between all fluorescence peaks and individual integrated NMR regions in the whole fluorescence (Table 10). A strong correlation ($P < 0.001$) exists in all regions of the whole fraction of the A and C peaks for all NMR integration areas. The aromatic region has a lesser correlation ($P < 0.02$) in the M peak. In the T peak, a lesser correlation ($P < 0.01$) exists with the CH_2 region. In the reconstituted fraction, a strong correlation of ($P < 0.001$) exists in all region except the aromatic region (Table 11). Comparing the slopes of the individual fluorescence peaks vs the integral values of individual NMR regions (Δ Fluorescence/ Δ NMR integration), the greatest contributor to the fluorescence is the Ar-H region (Table 10 and 11). When the individual peaks are compared to the total fluorescence the same trend is apparent, the Ar-H region is the smallest contributor to the total NMR integration (Figure 5), but it is the largest contributor to the fluorescence, suggesting that the Ar-H region is responsible for most of the fluorescence.

Impact of Storm Origin

Rain events were subdivided as either terrestrial or marine in order to determine influence of storm origin on the amount and composition of DOM in rainwater. NMR data further explains how storm origin influences the composition of DOM in rain. Total Fluorescence vs NMR integral regions were compared for marine rains vs terrestrial rains. The only and strongest correlation in the marine samples (Table 8) exists in the Ar-H region. Interestingly, in marine rains, the aromatic region is the only region that showed significant correlation ($P<0.1$) between

fluorescence and NMR integration values, but the aromatic region is the only NMR region that shows no correlation with fluorescence in the terrestrial storms (Table 9).

Table 6. Slope, R value, and P value for whole and reconstituted fluorescence values compared to respective integrations areas from NMR analysis. n= number of samples

Integration Area n=36	Slope Whole	R value Whole	P value Whole	Slope Reconstituted	R value Reconstituted	P value Reconstituted
Total	1605.0	0.790	<0.001	505.14	0.761	<0.001
Ar-H	49691	0.393	<0.02	16727	0.405	<0.02
CH-O	8001.4	0.804	<0.001	2472.5	0.761	<0.001
CH-C=	4888.9	0.753	<0.001	1571.7	0.741	<0.001
CH_2	4000.7	0.778	<0.001	1245.7	0.742	<0.001
CH_3	14704	0.743	<0.001	4674.0	0.723	<0.001

Table 7. Slope, R value, and P value for whole and reconstituted DOC values compared to respective integrations areas from NMR analysis. n= number of samples

Integration Area n=17	Slope Whole x 10^3	R value Whole	P value Whole	Slope Reconstituted	R value Reconstituted x 10^3	P value Reconstituted
Total	136	0.729	<0.001	0.4565	756	<0.001
Ar-H	0.200	0.064	<0.1	0.0063	543	<0.02
CH-O	27.0	0.702	<0.01	0.0982	795	<0.001
CH-C=	41.0	0.728	<0.001	0.1367	754	<0.001
CH_2	51.8	0.716	<0.001	0.1649	708	0.001
CH_3	16.6	0.747	<0.001	0.0504	703	<0.01

Table 8. Slope, R value, and P value for whole and reconstituted fluorescence values of Marine storms compared to respective integrations areas from NMR analysis. n= number of samples

Integration Area n=4	Slope Whole	R value Whole	P value Whole	Slope Reconstituted	R value Reconstituted	P value Reconstituted
Total	-1188.4	0.618	>0.1	-466.64	0.464	>0.1
Ar-H	241815	0.872	<0.1	119548	0.824	<0.1
CH-O	13147	0.429	>0.1	5482.5	0.341	>0.1
CH-C=	-2942.2	0.721	>0.1	-1207.7	0.565	>0.1
CH_2	-2794.2	0.679	>0.1	-1122.2	0.521	>0.1
CH_3	2203.9	0.079	>0.1	3935.6	0.270	>0.1

Table 9. Slope, R value, and P value for whole and reconstituted fluorescence values of Terrestrial storms compared to respective integrations areas from NMR analysis. n= number of samples

Integration Area n=14	Slope Whole	R value Whole	P value Whole	Slope Reconstituted	R value Reconstituted	P value Reconstituted
Total	1440.8	0.744	<0.01	440.39	0.650	<0.01
Ar-H	41395	0.435	>0.1	14136	0.424	>0.1
CH-O	9167.7	0.782	<0.001	2973.6	0.724	<0.01
CH-C=	4289.1	0.757	<0.01	1270.4	0.641	0.01
CH_2	3300.7	0.710	<0.01	990.24	0.608	<0.02
CH_3	10134	0.517	<0.05	3373.6	0.492	<0.1

Table 10. Slope, R value, and P value for whole fluorescence values of peaks A, C, M, and T compared to respective integrations areas from NMR analysis. n= number of samples

Whole	A peak	A peak	A peak	C peak	C peak	C peak	M peak	M peak	M peak	T peak	T peak	T peak
Integration Area n=36	slope	R value	P value	slope	R value	P value	slope	R value	P value	slope	R value	P value
Total	248.9	0.743	<0.001	108.2	0.688	<0.001	227.2	0.791	<0.001	84.88	0.546	<0.001
Ar-H	6653	0.842	<0.001	2894	0.306	<0.100	6768	0.392	<0.020	4813	0.515	<0.001
CH-O	1251	0.765	<0.001	561.3	0.732	<0.001	1090	0.778	<0.001	468.2	0.618	<0.001
CH-C=	738.1	0.691	<0.001	313.7	0.626	<0.001	700.4	0.765	<0.001	264.9	0.535	<0.001
CH2-	624.0	0.734	<0.001	270.6	0.679	<0.001	575.4	0.789	<0.001	186.8	0.474	<0.010
CH3-	2317	0.716	<0.001	1016	0.669	<0.001	1977	0.712	<0.001	818.5	0.545	<0.001

Table 11. Slope, R value, and P value for reconstituted fluorescence values of peaks A, C, M, and T compared to respective integrations areas from NMR analysis. n= number of samples

Resonstituted	A peak	A peak	A peak	C peak	C peak	C peak	M peak	M peak	M peak	T peak	T peak	T peak
Integration Area n=36	slope	R value	P value	slope	R value	P value	slope	R value	P value	slope	R value	P value
Total	86.33	0.740	<0.001	31.62	0.752	<0.001	46.46	0.703	<0.001	31.66	0.610	<0.001
Ar-H	2898	0.413	<0.020	1009	0.399	<0.020	1550	0.390	<0.020	1460	0.468	<0.010
CH-O	426.5	0.749	<0.001	155.3	0.752	<0.001	219.7	0.682	<0.001	154.4	0.611	<0.001
CH-C=	264.0	0.710	<0.001	97.83	0.730	<0.001	145.2	0.690	<0.001	100.3	0.607	<0.001
CH2-	213.1	0.720	<0.001	77.87	0.730	<0.001	115.8	0.691	<0.001	75.99	0.578	<0.001
CH3-	794.7	0.705	<0.001	287.8	0.709	<0.001	420.4	0.659	<0.001	287.9	0.575	<0.001

Alkyl protons (Figure 4a) are the majority of the protons of C_{18} extracted material for both storm types with a greater integration in the terrestrial storm while the aromatic region offers the smallest integration. A greater percentage of protons in the Ar-H region (Figure 4b) are evident in the marine originated vs terrestrial storm while only contributing a small percentage (1-3%) of the overall integral percentages. However, the aromatic region is the biggest contributor to fluorescence. Figure 7 represents the entire data set of terrestrial and marine storms showing again that alkyl protons are the majority of the protons of C_{18} extracted material and do not vary by storm origin. Again, the aromatic region is the greatest contributor to fluorescence and does vary by storm origin.

The NMR analysis indicates that DOM collected from marine and terrestrial storms are compositionally different and this data is supported with fluorescence, Uv-Vis absorbance, and Doc data. A greater percent fluorescent DOC was present in the reconstituted fraction compared to terrestrial indicating that the reconstituted fraction likely contains aromatic DOC, supporting the NMR findings. The spectral slope in the reconstituted fraction was lower in the terrestrial derivded rains relative to the marine derived. The DOC concentration was higher in the terrestrial derived rains relative to marine. More DOC was reconstituted in marine storms possibly because of the more recalcitrant, hydrophobic, and higher molecular weight matter. This may explain the background DOC of 20 μM observed in all marine rains. Higher DOC in terrestrial storms is due to the storm having more organic acids which will pass through the C_{18} cartridge because they are hydrophilic, thus not being retained on the cartridge. Relative abundance of DOM as a fraction of DOC increases in marine storms because the hydrophilic portion has been removed.

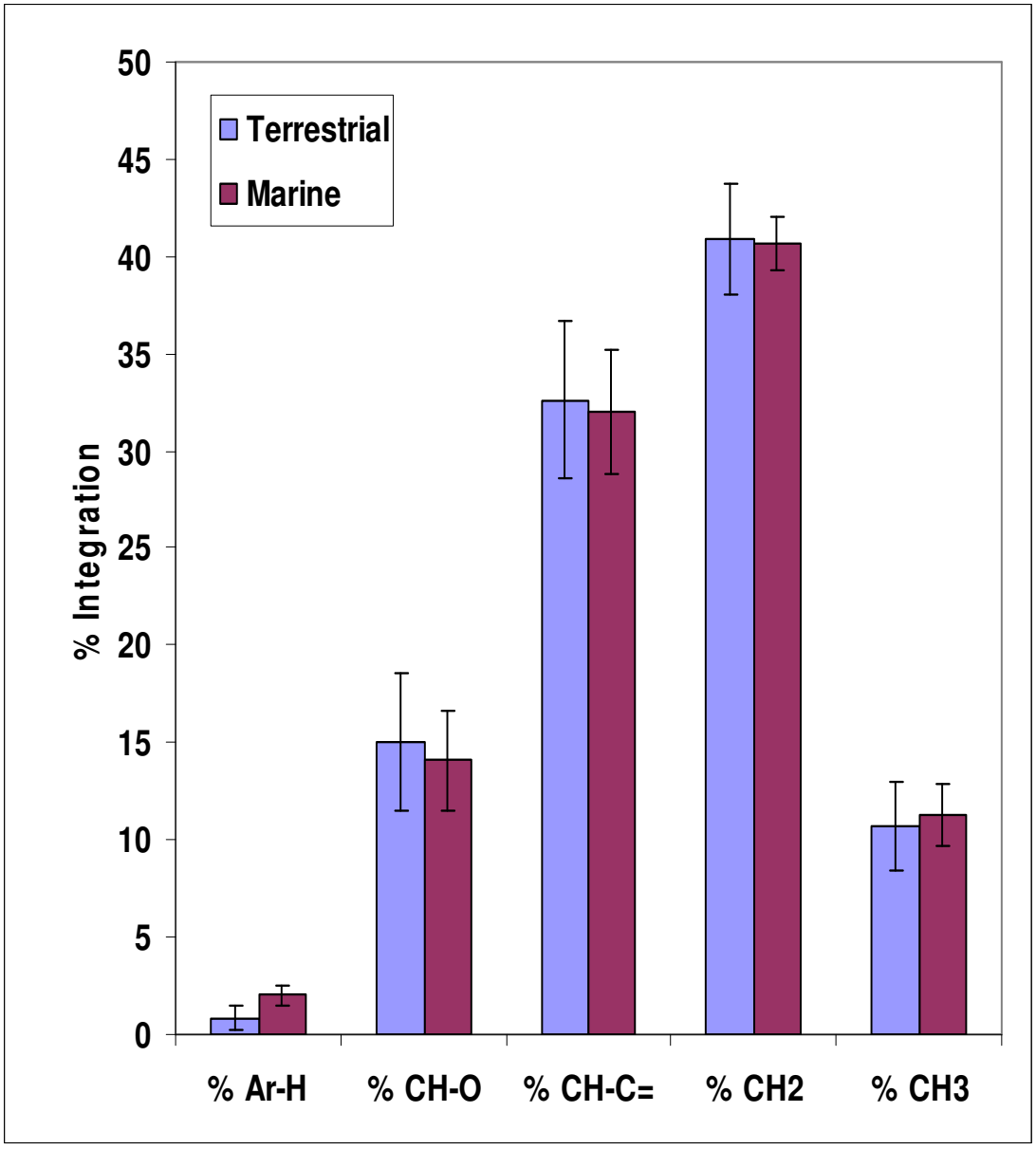

Figure 7. Average of respective integrated regions and % integration of respective NMR regions for all marine and terrestrial originated storms with standard deviations.

Seasonality

All rain events were separated into warm and cold seasons in order to determine the impact of season on the variability of DOM in rainwater. The warm and cold seasons correspond to the growing and non-growing seasons. The warm season was defined as April 1 to September 31, while the cold season was defined as October 1 to March 31. The DOC concentration in rainwater collected during the warm season (137μM) is larger relative to cold season rainwater (40 μM) (Table 3a). The concentrations ranged from47.1 to 599 μM for the warm season and 29.6 to 49.4 μM for the cold season (Table 3b). The % DOC reconstituted varied seasonally, 35 and 75% for the warm and cold season respectively, indicating a compositional difference in the DOC. The percentage DOC ranged from 12.8 to 75.7% and 26.8 to 126% respectively for the warm and cold seasons. This compositional difference is also supported with the spectral slope data. Both the whole and reconstituted samples had a higher slope in the warm season. The same pattern was reported previously in Kieber et al. (2006). Lower molecular weight is present in the summer due to higher organic acids which are known as DOM photodegredation products that can compromise as much as 45% of the DOC pool in rain. This indicates a shift to lower molecular weight DOM in summer months.

In summary, the objectives of my thesis were to quantify DOM UV-Vis absorbance and fluorescence in authentic and fractionated rainwater samples collected during different seasons and different storm types and to evaluate structural characteristics of rainwater DOM. Fluorescence, UV-Vis absorbance, and DOC concentrations, whole and fractionated, were measured in rainwater collected in Wilmington, NC, between September 15, 2005 to September 6, 2006. The concentration of DOC in rain varied between 30 and 599 μM and on average approximately half of the DOC was present in the C_{18} extractable fraction of the rainwater.

While all rain events contained fluorescent DOC, approximately half of the fluorescent DOC was present in the C_{18} filtrate fraction of the rainwater which contains the more hydrophobic portion of the DOC. This was not expected since it was previously thought that a majority of chromophoric DOC would be retained by the C_{18} cartridge. The C_{18} extractable DOC has been shown as an important complexor of metals, so understanding the composition of DOC in this fraction is important. Since half of the chromophoric DOC is present in the hydrophilic portion of the rain, the DOC is also important since the DOM in this fraction of rainwater will attenuate light in the atmosphere.

NMR spectra of the C_{18} extractable DOM in rainwater provided structural information about the DOM. A majority of the protons in the C_{18} extractable DOM are bound to alkyl carbons, but the aromatic region of the NMR spectra appears to be the region which changes the most dramatically between storms. The overall abundance of aromatic protons does not change between storms, but the contribution of protons in this region to the overall integration of the NMR spectra does change. In marine storms the aromatic protons are a more significant contributor to the overall NMR spectra integration compared to terrestrial storms. Marine storms also have lower DOC concentrations, lower spectral slopes, and a larger percent of the fluorescent material in the C_{18} extractable fraction of the rainwater. It has been observed that marine rainwater collected from remote sites have a DOC concentration of 20μM. This background DOM could be the aromatic, large molecular weight DOM which I observed in my marine rainwater samples. As a result of the aromaticity and large molecular weight this Dom might be recalcitrant and globally distributed.

Further studies will be conducted to examine the photodegredation of DOC in rainwater as well as additional characterization of DOC via NMR analysis. Stable and radiocarbon isotope analysis of rainwater will also be conducted.

REFERENCES

Aiken, G. R., D. M. McKnight, et al. (1985). Humic Substances in Soil, Sediment, and Water. Geochemistry, Isolation, and Characterization. New York, John Wiley & Sons.

Alvarez-Salgado, X. A. and A. E. J. Miller (1998). "Simultaneous determination of dissolved organic carbon and total dissolved nitrogen in seawater by high temperature catalytic oxidation: conditions for precise shipboard measurements." Marine Chemistry 62: 325-333.

Amador, J. A., P. J. Milne, et al. (1989). "Extraction of Chromophoric Humic Substances from Seawater." Marine Chemistry 29: 1-17.

Bruland, K.W. (1980). Oceanographic distributions of cadmium, zinc, nickel, and copper in the north pacific. Earth Planet. Sci. Lett. 47: 176-198.

Bruland, K.W., R.P. Franks, et al. (1979). "Sampling and analytical methods for the determination of copper, cadmium, zinc, and nickel at the nanogram per liter level in seawater." Anal. Chim. Acta 105: 223-245.

Capiello, A. et al. (2003) "Molecular characterization of the water soluble organic compounds in fogwater by ESIMS/MS." Environ. Sci. Technol. 37: 1229-1240.

Coble, P. G. (1996). "Characterization of marine and terrestrial DOM in seawater using excitation-emission matrix spectroscopy." Marine Chemistry 51: 325-346.

Coble, P. G., C. E. Del Castillo, et al. (1998). "Distribution and optical properties of DOM in the Arabian Sea during the 1995 Southwest Monsoon." Deep-Sea Research II 45: 2195-2223.

Coble, P. G., C. Schultz, et al. (1993). "Fluorescence contouring analysis of DOC Intercalibration Experiment samples: a comparison of techniques." Marine Chemistry 41: 173-178.

Decesari, S., M. C. Facchini, et al. (2002). "Water soluble organic compounds formed by oxidation of soot." Atmospheric Environment 36: 1827-1832.

DeHaan, H. (1993). "Solar UV-light penetration and photodegredation of humic substances in peaty lake water." Limnol. Ocenography 38: 1072-1076.

Del Castillo, C. E., P. G. Coble, et al. (1999). "Analysis of the optical properties of the Orinoco River plume by absorption and fluorescence spectroscopy." Marine Chemistry 66: 35-51.

Kieber, R. J., et al. (2006). "Chromophoric dissolved organic matter (DOM) in rainwater, southeastern North Carolina, USA." Journal of Atmospheric Chemistry. In press.

Kim, S. A. J. Simpson, et al. (2003). "High resolution electrospray ionization mass spectrometry and 2D solution NMR for the analysis of DOM extracted by $_{C18}$ solid phase disk." Organic Geochemistry. 34: 1325-1335.

Kuo, C. Y., T. C. Hung, et al. (1993). "Extraction, isolation, and purification of humic substances." Bull. Inst. Chem. Acad. Sin. 40: 91-103.

Merriam, J., W. H. McDowell, et al. (1996). "A High-Temperature Catalytic Oxidation Technique for Determining Total Dissolved Nitrogen." Journal of Soil Sci. Soc. Am. 60(July-August): 1050-1055.

Simjouw, J.P., C.E. Minor, et al. (2005). "Isolation and characterization of estuarine dissolved organic matter: comparison of ultrafiltration and $_{C18}$ solid-phase extraction techniques." Marine Chemistry. 96: 219-235.

Strome, D. J. and Miller, M. C. (1978). "Photolytic changes in dissolved humic substances." Limnol. Oceanography. 20: 1248-1254.

Werner, M. H. (1994). Bruker Avance User's Guide. Fallanden, Switzerland: 1-165.

Willey, J. D., R. J. Kieber, et al. (2000). "Rainwater dissolved organic carbon: Concentrations and global flux." Global Biogeochemical cycles 14(1): 139-148.